International Journal of Engineering Research-Online
A Peer Reviewed International Journal
Email:editorijoer@gmail.com http://www.ijoer.in

Vol.4., S1., 2016

N C L A – 2016

ISSN: 2321-7758

SYSTEMATIC STUDY OF INTER-COMBINATION LINES OF H-LIKE TO O-LIKE Cu & Kr

Y.G. Mulye*

Department of Physics, Finolex Academy of Management & Technology, Ratnagiri.

*E-mail:yogesh_mulye@rediffmail.com

ABSTRACT

Multi-configuration Dirac-Fock (MCDF) calculations have been carried out in the Extended Optimal Level (EOL) scheme on energies, transition probabilities and weighted absorption oscillator strengths of intercombination lines of highly ionized Cu and Kr. The calculations have been carried out with empty K shell, varying degrees of ionization in the L shell and open outer shells. The radiative transition rates have been calculated in both length and velocity gauges. The transition rates in length and velocity forms have been compared to analyse accuracy of orbital functions.

Keywords: Multi-configuration Dirac-Fock, Self-Consistent Field.

1. INTRODUCTION

The inter-combination lines are spin-forbidden lines and arise due to$\Delta S \neq 0$. These transitions are purely forbidden in LS coupling. The spin-forbidden electric dipole transitions are of great importance in diagnostics of different astrophysical sources. These lines can be observed experimentally with high resolution spectrograph in the spectra of light elements.

The inter-combination lines in some He-like to O-like isoelectronic sequence have been studied both theoretically and experimentally [1-6]. All these data correspond to single ionization in the K shell. In our earlier work [7], we reported our relativistic calculation on inter-combination lines of argon with single ionization in K shell and multiple ionization in L shell and open outer shells. However, no systematic relativistic calculation on spin forbidden lines of atoms ionized doubly K shell exist. Recently, we have reported MCDF calculations on the various electric dipole spin allowed and spin forbidden transitions of argon with doubly excited K shell and multiply ionized L shell [7-10]. In this paper, we present a complete set of calculationsof the transition parameters for all the electric dipole spin forbidden lines in the $2s^a 2p^b \rightarrow 1s^1 2s^a 2p^{b-1}$ transitions of copper and Krypton. Here a and$b$ are occupation numbers of electrons in 2s and 2p sub shells respectively and a varies from 0 to 2 and b from 1 to 6. As the inter-combination lines are entirely due to relativistic effects and the transition rates are found to be sensitive to different correlation effects, in this work we have made use of MCDF wavefunctions and included some amount of correlation in the evaluation of radial wave functions. As the inter-combination transitions are gauge dependent, we calculated the radiative rates in both length and velocity forms thereby checking the accuracy of the wavefunctions employed in the evaluation of transition rates. The calculations have been carried out in EOL scheme with block structuring of the Hamiltonian. The graspVU package [11-12] is used to generate MCDF wavefunctions and perform the structure calculations.

2. THEORETICAL BACKGROUND

The relativistic MCDF computational program used in the evaluation of a large-scale atomic structure properties are described in detail elsewhere [11-14]. In the MCDF method, configuration state functions (CSFs) $\emptyset(\Gamma J^P)$ of a certain J and parity are formed by taking a linear

combination of Slater determinants of the Dirac orbitals. A linear combination of these CSFs is then used in the construction of atomic state functions (ASFs) with the same and J and parity.

$$\psi_i(J^P) = \sum_{\alpha=i}^{n_{csf}} c_{i\alpha}\, \emptyset(\Gamma_\alpha J^P) \qquad (1)$$

Where $c_{i\alpha}$ are the mixing coefficients for the state *i*, and n_{csf} is the number of CSFs included in the evaluation of ASF. The ASFs thus constructed were used in solving the Dirac-Fock equation and the Dirac-Coulomb Hamiltonian is

$$\hat{H}^{DC} = \sum_{i=1}^{N-1} \hat{H}_D(i) + \sum_{i=1}^{N-1}\sum_{j=i+1}^{N} \left|\hat{r}_i - \hat{r}_j\right|^{-1} \qquad (2)$$

where the first term is the one body contribution for an electron due to kinetic energy and interaction with the nucleus and can be expressed as

$$\hat{H}_D = c\hat{\alpha}\hat{p} + (\beta - 1)c^2 + V_{nuc}(r) \qquad (3)$$

Here the rest energy has been subtracted out. The two-body coulomb interactions between the electrons comprise the second term. The relativistic transition probabilities can be calculated using the Coulomb or Babushkin gauge, which in non-relativistic limit correspond to velocity and length form respectively [15]. For a multi-configuration model, the values of the electric multipole transition rates calculated in Coulomb gauge in general differ from those calculated using length gauges. The length and velocity forms of weighted absorption oscillator strengths in dipole approximation for transitions between initial and final states is given by

$$gf_l = \frac{2}{3}\left(E_i - Ef\psi ik{=}1Nrk\psi f \right. \qquad (4)$$

$$gf_v = \frac{2}{3(E_i - E_f)}\left|\langle\psi_i| \sum_{k=1}^{N} \nabla_k \,|\psi_f\rangle\right| \qquad (5)$$

Where ψ_i and ψ_f are normalised wavefunctions of initial and final states which corresponds to energies E_i and E_f. The summation takes into account all N electrons occupying a configuration and g is the statistical weight of initial state.

3. METHOD OF CALCULATION

In EOL scheme used in the present work, the energy functional is the weighted sum of the total energy corresponding to a set of ASFs defined by$\{\Gamma_\alpha J_\alpha\}$. As a starting point, using *jj* coupled states as basis, DF calculations were performed on the three sets of reference configurations: (1) $2p^b \rightarrow 1s2p^{b-1}$ (2) $2s2p^b \rightarrow 1s^1 2s2p^{b-1}$ (3) $2s^2 2p^b \rightarrow 1s^1 2s^2 2p^{b-1}$ with *b* varying from 1 to 6. Then the electron correlation effects were included by continuing the calculations in the active space expansion method. In this approach, the CSF of specific parity and angular momentum J are generated by a single and double electron substitution from the reference configurations to an active set that is increased in a systematic way taking into account the convergence of the expectation values. Following our earlier work [7], in the present paper also active set has comprised the orbitals {1s, 2s, 2p, 3s, 3p, 3d, 4s, 4p, 4d, 4f}. Our calculations showed that double excitation of the active set with n=4 gave well-converged orbital functions and energy eigenvalues[7]. These optimized orbitals were then used to evaluate the transition parameters. Details on the numerical calculations are given in our earlier paper [7]. In ref. [7], it is ensured that active space upto n=4 incorporates sufficient orbitals so that significant intra-shell correlations are included.

RESULT AND DISCUSSION

A number of MCDF calculations were carried out on the various initial and final states. Though the calculations were performed in *jj* coupling, the different transitions are denoted in the LS coupling scheme. The energies and transition rates calculated both in length and velocity gauges for all the possible inter-combination lines arising from initial configuration 2sa2pb of Cu and Kr with a=0 to 2 and b=1 to 6 are listed in Tables I to VI with Table I and III correspond to a=0, 1 and 2 respectively for Cu and Table IV, V and VI to a=0,1 and 2 for Kr. The weighted absorption oscillator strengths in length form are also listed in these tables. It may be noted that to the best of our knowledge no experimental data on the transitions considered in this work are available. In each table, the initial and final states are grouped according to the number of electrons in the 2p subshell and within each group, the transitions are arranged in

decreasing order of energy. For each line, we have included the initial and final terms in the first column of each table. Only those transitions for which the transition rates are $\geq 10^8 s^{-1}$ are included in this work to limit the length of the tables.

Table-I: Energies in eV and electric dipole rates in 10^{13} s^{-1} in length (A_l) and Coulomb (A_v) gauges and weighted absorption oscillator strength in 10^{-1} in length form of the inter-combination lines of Copper for $2p^b \rightarrow 1s2p^{b-1}$transitions.

Transition		Energy	A_l	A_v	gf_l
$2p^2 - 1s2p$					
$^1D_2$	$^3P_2$	8663.77	26.425	25.938	4.057
$^3P_2$	$^3P_1$	8612.66	18.443	19.636	2.865
$2p^3 - 1s2p^2$					
$^2D_{3/2}$	$^4P_{3/2}$	8619.69	13.727	13.303	1.703
$^2D_{5/2}$	$^4P_{5/2}$	8619.02	12.507	12.154	2.328
$2p^4 - 1s2p^3$					
$^1D_2$	$^3P_2$	8561.43	49.967	50.279	7.855
$^3P_1$	$^1D_2$	8526.97	23.359	24.413	2.221
$2p^5 - 1s2p^4$					
$^2P_{5/2}$	$^4P_{3/2}$	8523.71	17.762	17.641	2.254
$2p^6 - 1s2p^5$					
$^1S_0$	$^3P_1$	8479.10	55.028	54.629	1.764

Table-II: Energies in eV and electric dipole rates in 10^{13} s^{-1} in length (A_l) and Coulomb (A_v) gauges and weighted absorption oscillator strength in 10^{-1} in length form of the inter-combination lines of Copper for $2s2p^b \rightarrow 1s2s2p^{b-1}$transitions.

Transition		Energy	A_l	A_v	gf_l
$2s2p^3 - 1s2s2p^2$					
$^1D_2$	$^3D_1$	8551.24	61.738	62.276	9.729
$^1D_2$	$^3D_2$	8547.73	13.839	14.006	2.183
$^3S_1$	$^1D_2$	8541.16	14.359	14.641	1.361
$^1D_2$	$^3D_3$	8538.22	27.625	28.705	4.367
$2s2p^4 - 1s2s2p^3$					
$^2P_{1/2}$	$(^1S)\ ^4S_{3/2}$	8539.57	11.879	11.860	7.508
$^2D_{5/2}$	$^4P_{5/2}$	8535.88	13.141	12.914	2.494
$^2D_{3/2}$	$(^1S)\ ^4S_{3/2}$	8515.63	57.481	58.338	7.307
$2s2p^5 - 1s2s2p^4$					
$^1P_1$	$(^1S)\ ^3P_2$	8491.04	28.006	27.451	2.686

Table-III: Energies in eV and electric dipole rates in 10^{13} s^{-1} in length (A_l) and Coulomb (A_v) gauges and weighted absorption oscillator strength in 10^{-1}in length form of the inter-combination lines of Copper for $2s^2 2p^b \rightarrow 1s2s^2 2p^{b-1}$transitions.

Transition		Energy	A_l	A_v	gf_l
$2s^2 2p^2 - 1s2s^2 2p$					
$^1D_2$	$^3P_2$	8583.13	25.024	23.976	3.914
$^3P_2$	$^1P_1$	8534.18	17.515	18.194	2.771
$2s^2 2p^3 - 1s2s^2 2p^2$					
$^2D_{3/2}$	$^4P_{3/2}$	8542.17	12.518	11.843	1.581
$^2D_{5/2}$	$^4P_{5/2}$	8541.42	11.829	11.226	2.242

$2s^2 2p^4 - 1s2s^2 2p^3$					
$^1D_2$	$^3P_2$	8486.95	49.753	49.385	7.959
$^3P_1$	$^1D_2$	8453.65	23.017	23.671	2.227
$2s^2 2p^5 - 1s2s^2 2p^4$					
$^2P_{3/2}$	$^4P_{3/2}$	8451.39	16.464	15.934	2.125
$2s^2 2p^6 - 1s2s^2 2p^5$					
$^1S_0$	$^3P_1$	8479.10	55.028	54.629	1.764

Table-IV: Energies in eV and electric dipole rates in 10^{13} s^{-1} in length (A_l) and Coulomb (A_v) gauges and weighted absorption oscillator strength in 10^{-1} in length form of the inter-combination lines of Krypton for $2p^b \rightarrow 1s2p^{b-1}$transitions.

Transition		**Energy**	**A_l**	**A_v**	**gf_l**
$2p^2 - 1s2p$					
$^1D_2$	$^3P_2$	13467.76	83.017	81.561	5.274
$^3P_2$	$^1P_1$	13370.83	51.072	55.406	3.292
$2p^3 - 1s2p^2$					
$^2D_{3/2}$	$^4P_{3/2}$	13407.76	63.124	61.669	3.237
$^2D_{5/2}$	$^4P_{5/2}$	13406.77	57.625	56.381	4.433
$2p^4 - 1s2p^3$					
$^3P_2$	$^5S_2$	13352.09	43.907	42.127	2.838
$^1D_2$	$^3P_2$	13336.98	152.249	152.328	9.863
$^3P_1$	$^1D_2$	13264.46	73.128	78.154	2.874
$2p^5 - 1s2p^4$					
$^2P_{3/2}$	$^4P_{3/2}$	13280.43	123.894	123.894	6.476
$2p^6 - 1s2p^5$					
$^1S_0$	$^3P_1$	13227.15	238.315	236.858	3.139

Table-V: Energies in eV and electric dipole rates in 10^{13} s^{-1} in length (A_l) and Coulomb (A_v) gauges and weighted absorption oscillator strength in 10^{-1} in length form of the inter-combination lines of Krypton for $2s2p^b \rightarrow 1s2s2p^{b-1}$transitions.

Transition		**Energy**	**A_l**	**A_v**	**gf_l**
$2s2p^2 - 1s2s2p$					
$^2D_{5/2}$	$^4P_{5/2}$	13428.17	49.284	47.177	3.779
$^4P_{5/2}$	$(^1S)\ ^2P_{3/2}$	13308.81	28.173	30.606	2.199
$2s2p^3 - 1s2s2p^2$					
$^3D_2$	$^5P_2$	13373.11	33.855	31.892	2.181
$^1P_1$	$^3S_1$	13369.82	25.967	24.688	1.004
$^3S_1$	$^1D_2$	13274.01	21.368	22.557	0.838
$^3P_2$	$^1D_2$	13266.01	27.115	28.980	1.775
$^3P_2$	$^1P_1$	13259.30	41.088	43.984	2.693
$^3P_1$	$^1D_2$	13256.54	20.245	21.774	0.796
$2s2p^4 - 1s2s2p^3$					
$^4P_{5/2}$	$^6S_{5/2}$	13322.60	21.487	19.891	1.674
$^2P_{1/2}$	$(^1S)\ ^4S_{3/2}$	13303.53	42.238	41.254	1.100
$^2D_{5/2}$	$^4P_{5/2}$	13296.16	84.868	83.834	6.638
$^2D_{3/2}$	$(^3S)\ ^4S_{3/2}$	13291.60	97.269	96.282	5.075
$^2D_{3/2}$	$(^1S)\ ^4S_{3/2}$	13266.48	53.195	54.104	2.786

$^4P_{3/2}$	$^2D_{3/2}$	13208.68	28.753	30.918	1.519
$^4P_{3/2}$	$^2D_{5/2}$	13201.50	24.517	26.741	1.297
$2s2p^5 - 1s2s2p^4$					
$^3P_2$	$^5P_2$	13246.94	47.139	45.569	3.095
$^1P_1$	$(^1S)\ ^3P_2$	13246.20	101.241	98.248	3.989
$^1P_1$	$(^1S)\ ^3P_0$	13233.87	25.047	24.481	0.989
$^1P_1$	$^3S_1$	13222.85	95.987	96.146	3.796
$^3P_1$	$^1D_2$	13146.46	29.443	32.165	1.178
$^3P_0$	$^1P_1$	13143.50	62.732	67.659	0.837
$2s2p^6 - 1s2s2p^5$					
$^2S_{1/2}$	$^4P_{3/2}$	13199.39	64.749	61.904	1.713
$^2S_{1/2}$	$^4P_{1/2}$	13178.35	54.766	53.687	1.453

Table-VI: Energies in eV and electric dipole rates in 10^{13} s^{-1} in length (A_l) and Coulomb (A_v) gauges and weighted absorption oscillator strength in 10^{-1} in length form of the inter-combination lines of Krypton for $2s^2 2p^b \rightarrow 1s2s^2 2p^{b-1}$transitions.

Transition		**Energy**	**A_l**	**A_v**	**gf_l**
$2s^22p^2 - 1s2s^22p$					
$^1D_2$	$^3P_2$	13364.24	80.023	77.142	5.163
$^3P_2$	$^1P_1$	13271.03	49.483	52.629	3.237
$2s^22p^3 - 1s2s^22p^2$					
$^2D_{3/2}$	$^4P_{3/2}$	13307.37	60.544	58.051	3.152
$^2D_{5/2}$	$^4P_{5/2}$	13306.45	55.573	53.363	4.340
$^2S_{3/2}$	$^2P_{1/2}$	13218.85	33.551	35.761	1.770
$2s^22p^4 - 1s2s^22p^3$					
$^1D_2$	$^3D_3$	13259.43	30.063	29.005	1.970
$^3P_2$	$^5S_2$	13254.19	41.257	38.995	2.706
$^1D_2$	$^3P_2$	13239.48	147.55	145.834	9.700
$^1D_2$	$^3S_1$	13230.09	27.641	26.495	1.820
$^3P_1$	$^1D_2$	13169.34	71.135	75.092	2.836
$2s^22p^5 - 1s2s^22p^4$					
$^2P_{3/2}$	$^4P_{3/2}$	13185.43	119.402	116.997	6.331
$2s^22p^6 - 1s2s^22p^5$					
$^1S_0$	$^3P_1$	13227.15	238.315	236.858	3.139

It is seen from each table that the energies of the inter-combination lines from each group with a given value of b shows distinct structures. However, the energies of the photons from groups with different b values overlap in general.

Table VII: Analysis of Nature of spectra of Cu and Kr for Tables I to VI for various transitions for different values of b.

Element	**Table No**	**Transition**	**Values of b**	**Nature of spectra**
Cu	I	$2p^b \rightarrow 1s2p^{b-1}$	2, 3	Overlap
			4, 5	Overlap
			6	Distinct
Cu	II	$2s2p^b \rightarrow 1s2s2p^{b-1}$	3, 4	Overlap
			5	Distinct

Cu	III	$2s^2 2p^b \rightarrow 1s2s^2 2p^{b-1}$	2, 3	Overlap
			4, 6	Overlap
			5	Distinct
Kr	IV	$2p^b \rightarrow 1s2p^{b-1}$	2, 3	Overlap
			4, 5	Overlap
			6	Distinct
Kr	V	$2s2p^b \rightarrow 1s2s2p^{b-1}$	2, 3, 4, 5, 6	Clustered
Kr	VI	$2s^2 2p^b \rightarrow 1s2s^2 2p^{b-1}$	2, 3, 4, 5, 6	Clustered

No inter-combination lines are generated for b=1 and for any value of '*a*' for both Cu and Kr. However, no inter-combination lines are seen in Table II corresponding to b=2 and 6.A comparison done in Table-VII confirms the overlapping structure of inter-combination lines.

The transition rates listed in Tables I to VI confirms our earlier analysis that the length form of rates are larger than the rates in coulomb gauge for some transitions and are smaller for other transitions. For Cu difference between length gauge and velocity gauge varies between -6.1% to +5.7% and for Kr variation is in the range -8.5% to +8%. It is seen from Table-I to VI that for b=5, 6 transition rates in length gauge are larger than velocity gauge for all transitions except for a=1 and b=5 for both the elements Cu and Kr.

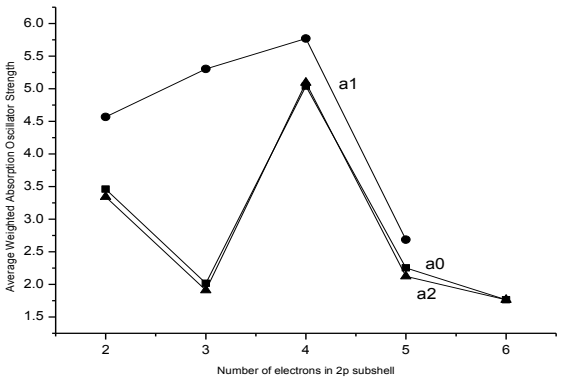

Figure-1: A graph of Average Weighted Oscillator Strength in length form in 10-1 versus Number of electrons in 2p subshell for Cupper.

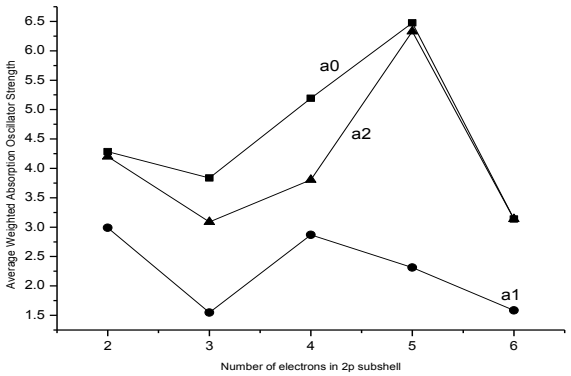

Figure-2: A graph of Average Weighted Oscillator Strength in length form in 10-1 versus Number of electrons in 2p subshell for Krypton.

Mean values of weighted absorption oscillator strengths for a=0 to 2 and b=1 to 6 for transitions in Cu and Kr are plotted as a function of number of electrons in 2p subshell. The symbols a0, a1, a2 correspond to the number of electrons in the 2s subshell. It is seen from the plot that trends of the curvea1 is different from that of a0 and a2 for both Cu and Kr.

CONCLUSION

Systematic relativistic calculations on the transition parameters of various states of $2p^b, 2s2p^b \; and \; 2s^2 2p^b$ configurations of Cu and Kr with b varying from 1 to 6 have been performed in MCDF formalism. As no other experimental or theoretical data on the complete set of fine structure lines reported in this work are available it is not possible to fully assess the accuracy of the present values. The results of this work could guide in analysing the experimentally observed high-resolution spectra.

References

[1]. Hibbert, A. (1979). The 2s3p 3P1-2s2 1S0 intercombination line in the beryllium sequence. Journal of Physics B: Atomic and Molecular Physics,12(22), L661.

[2]. Fleming, J., Hibbert, A., & Stafford, R. P. (1994). The 1909 Å intercombination line in C III. PhysicaScripta, 49(3), 316.

[3]. Ynnerman, A., & Fischer, C. F. (1995). Allowed transitions and intercombination lines in B II. ZeitschriftfürPhysik D Atoms, Molecules and Clusters, 34(1), 1-8.

[4]. Ynnerman, A., & Fischer, C. F. (1995). Multiconfigurational-Dirac-Fock calculation of the 2s21S0–2s2p 3P1 spin-forbidden transition for the Be-like isoelectronic sequence. Physical Review A, 51(3), 2020.

[5]. Curtis, L. J., & Ellis, D. G. (1996). Predictive systematization of line strengths for the resonance and intercombination transitions in the Be isoelectronic sequence. Journal of Physics B: Atomic, Molecular and Optical Physics, 29(4), 645.

[6]. Cook, J. W., Keenan, F. P., Dufton, P. L., Kingston, A. E., Pradhan, A. K., Zhang, H. L., & Hayes, M. A. (1995). The O IV and S IV intercombination lines in solar and stellar ultraviolet spectra. The Astrophysical Journal, 444, 936-942.

[7]. Mulye, Y. G., & Natarajan, L. (2004). Systematic studies on the Inter-combination lines of He-like to O-like argon. PhysicaScripta, 69(1), 24.

[8]. Natarajan, L., &Mulye, Y. G. (2001). Multi-configuration Dirac-Fock and configuration-interaction calculations of Ar7+ to Ar17+ ions. Journal of Physics B: Atomic, Molecular and Optical Physics, 34(9), 1839.

[9]. Mulye, Y. G., & Natarajan, L. (2005). Relativistic transition rates for dipole lines of multiply ionized argon. Journal of Quantitative Spectroscopy and Radiative Transfer, 94(3), 477-489.

[10]. Natarajan, L. (2002). Spin-forbidden electric dipole transitions of highly ionized argon. Journal of Physics B: Atomic, Molecular and Optical Physics,35(14), 3179.

[11]. Jönsson, P., He, X., Fischer, C. F., (Private Communication)

[12]. Parpia, F. A., Fischer, C. F., & Grant, I. P. (1996). GRASP92: A package for large-scale relativistic atomic structure calculations. Computer physics communications, 94(2), 249-271.

[13]. Jönsson, P., He, X., Fischer, C. F., & Grant, I. P. (2007). The grasp2K relativistic atomic structure package. Computer Physics Communications,177(7), 597-622.

[14]. Dyall, K. G., Grant, I. P., Johnson, C. T., Parpia, F. A., & Plummer, E. P. (1989). GRASP: A general-purpose relativistic atomic structure program.Computer physics communications, 55(3), 425-456.

[15]. Grant, I. P. (1974). Gauge invariance and relativistic radiative transitions.Journal of Physics B: Atomic and Molecular Physics, 7(12), 1458